Carbohydrate Polymers 114 (2014) 416–423

Contents lists available at ScienceDirect

Carbohydrate Polymers

journal homepage: www.elsevier.com/locate/carbpol

Surface esterification of cellulose nanofibers by a simple organocatalytic methodology

Jhon Alejandro Ávila Ramírez[a,b], Camila Juan Suriano[a], Patricia Cerrutti[a,c], María Laura Foresti[a,b,*]

[a] Grupo de Biotecnología y Biosíntesis—Instituto de Tecnología en Polímeros y Nanotecnología (ITPN)—Facultad de Ingeniería, Universidad de Buenos Aires, Las Heras 2214 (CP 1127AAR), Buenos Aires, Argentina
[b] Consejo Nacional de Investigaciones Científicas y Técnicas (CONICET), Argentina
[c] Departamento de Ingeniería Química, Facultad de Ingeniería, Universidad de Buenos Aires, Argentina

ARTICLE INFO

Article history:
Received 12 June 2014
Received in revised form 11 August 2014
Accepted 17 August 2014
Available online 23 August 2014

Keywords:
Bacterial cellulose
Surface esterification
Organocatalysis
Characterization

ABSTRACT

Bacterial cellulose nanofibers were esterified with two short carboxylic acids by means of a simple and novel organic acid-catalyzed route. The methodology proposed relayed on the use of a non-toxic biobased α-hydroxycarboxylic acid as catalyst, and proceeded under moderate reaction conditions in solventless medium. By varying the esterification interval, acetylated and propionized bacterial cellulose nanofibers with degree of substitution (DS) in the 0.02–0.45 range could be obtained. Esterified bacterial cellulose samples were characterized by means of Solid-State CP/MAS ^{13}C Nuclear Magnetic Resonance spectroscopy (CP/MAS ^{13}C NMR), Fourier Transform Infrared spectroscopy (FTIR), X-ray Diffraction (XRD), Thermogravimetric Analysis (TGA) and chosen hydrophobicity test assays. TGA results showed that the esterified nanofibers had increased thermal stability, whereas XRD data evidenced that the organocatalytic esterification protocol did not alter their crystallinity. The analysis of the ensuing modified nanofibers by NMR, FTIR, XRD and TGA demonstrated that esterification occurred essentially at the surface of bacterial cellulose microfibrils, something highly desirable for changing their surface hydrophilicity while not affecting their ultrastructure.

1. Introduction

Cellulose is the main component of wood and most natural fibers, and it is also produced by tunicates and certain bacteria. In the last decade, cellulose microfibrils and cellulose nanocrystals obtained from the mentioned sources have received increasing attention based on their unique properties such as high water holding capacity, high crystallinity, low thermal expansion coefficient in the axial direction, and high tensile strength and Young modulus. Among nanocellulose applications, its use as reinforcement of nanocomposites is a continuously growing field (Hubbe, Rojas, Lucia, & Sain, 2008; Siro & Plackett, 2010; Siqueira, Bras, & Dufresne, 2010). The relative low cost, low density, availability, renewability and environmentally benign character of cellulose, as well as the proved high mechanical properties of nanocellulosics, have encouraged their use as matrix reinforcement. However, the highly polar surface of native cellulose nanoparticles associated with their OH-rich structure leads to low interfacial compatibility with non-polar matrices which results in inadequate mechanical performance of the corresponding composites; high moisture uptake which leads to loss of fiber strength and composite deformation; and inter-fiber aggregation by hydrogen bonding which results in poor fiber dispersion in the composite (Ifuku et al., 2007; Tomé et al., 2011; Yuan, Nishiyama, Wada, & Kuga, 2006; Berlioz, Molina-Boisseau, Nishiyama, & Heux, 2009).

To overcome the mentioned difficulties, chemical modification of cellulose nanofibers can be attempted. In particular, esterification reactions in which an acylant reacts with the hydroxyl groups of cellulose nanofibers to produce less hydrophilic ester groups is a common technique used to turn the cellulose surface into a more hydrophobic one. Esterification of cellulose nanofibers can be accomplished by use of homogeneous or heterogeneous processes. In the homogeneous mechanism, mainly applied in cellulose acetylation processes, the esterified cellulose microfibrils are soluble in the medium, and thus the chains located at the cellulose surface diffuse into the surrounding solvent as soon as they are substantially derivatized (Sassi & Chanzy, 1995). On the other hand, in the heterogeneous or "fibrous" process, esterification is carried out in a

* Corresponding author. Tel.: +54 11 45143010; fax: +54 11 45143010.
E-mail address: mforesti@fi.uba.ar (M.L. Foresti).

http://dx.doi.org/10.1016/j.carbpol.2014.08.020
0144-8617/

medium that is a nonsolvent for both native and esterified cellulose; and cellulose nanofibers morphology is preserved (Berlioz et al., 2009). In the last decade, different heterogeneous methodologies for the esterification of cellulose nanoparticles have been proposed, including acetylation of compressed bacterial cellulose pellicles catalyzed by perchloric acid in toluene medium (Ifuku et al., 2007), surface acylation of cellulose whiskers with alkyenyl succinic anhydride aqueous emulsion followed by heat annealing (Yuan et al., 2006), solvent-free gas-phase esterification of cellulose whiskers and bacterial cellulose microfibrils with palmitoyl chloride (Berlioz et al., 2009), simultaneous isolation and Fischer esterification of hydroxyl groups of cellulose nanowhiskers in aqueous medium using acetic and butyric acids (Braun & Dorgan, 2009), heterogeneous esterification of cellulose whiskers with long-chain fatty acids in p-tosyl chloride/pyridine medium (Uschanov, Johansson, Maunu, & Laine, 2011), solvent-free acetylation of bacterial cellulose using acetic anhydride in the presence of iodine as a catalyst (Hu, Chen, Xu, & Wang, 2011), and heterogeneous esterification of bacterial cellulose using ionic liquids as solvent media and catalysts (Tomé et al., 2011), among others.

In the current manuscript, bacterial nanocellulose (BNC) was heterogeneously esterified in the absence of solvents using an operationally simple eco-friendly methodology. Esterification with acetic and propionic acids as acylants was accomplished by use of an organic-acid-catalyzed heterogeneous route developed by Hafrén and Córdova (2005) for the organocatalytic ring-opening polymerization of ε-caprolactone from cotton and paper cellulose. The mentioned authors also applied this route for the esterification of cotton fibers with hexadecanoic and pentynoic acids catalyzed by tartaric acid. The organocatalytic esterification methodology described has recently been applied to the synthesis of starch acetates and butyrates with varying acylation levels (Tupa, Maldonado, Vazquez, & Foresti, 2013). However, at the authors' best knowledge the esterification of cellulose nanofibers by use of the described organocatalytic route has not been reported before. Acetylated and propionized cellulose nanofibers obtained herein were characterized by means of CP/MAS ^{13}C NMR, FTIR, DRX, TGA and chosen hydrophobicity test assays, in order to demonstrate the suitability of the organic acid-catalyzed route for BNC esterification, and study the effect of derivatization on particular properties of BNC.

2. Materials and methods

2.1. Microorganism

The bacterial strain of *Gluconacetobacter xylinus* (syn. *Acetobacter aceti* subsp. *xylinus, Acetobacter xylinum*) NRRL B-42 used in this work was gently provided by Dr. Luis Ielpi (Fundación Instituto Leloir, Buenos Aires, Argentina).

2.2. Materials

Acetic acid (99.5%) and propionic acid (99.5%) were purchased from Dorwil. Hydrochloric acid (36.5–38%) and sodium hydroxide were reagent grade chemicals purchased from Anedra and BioPack, respectively. Potassium hydrogen phthalate and sodium carbonate were bought from Laboratorios Cicarelli and Mallinckrodt, respectively. For BNC production, anhydrous dextrose (Biopack), meat peptone and yeast extract (Britania, Laboratorios Britania S.A.), disodium phosphate (Anhedra), citric acid (Merck), glycerol (Sintorgan) and corn steep liquor (Ingredion) were used.

2.3. Bacterial cellulose production

Inocula were cultured for 48 h in Erlenmeyers flasks containing Hestrin and Schramm (HS) medium (%, w/v): glucose, 2.0; peptone, 0.5; yeast extract, 0.5; disodium phosphate, 0.27; citric acid, 0.115. The pH was adjusted to 6.0 with dil. HCl or NaOH. Agitation (200 rpm) was provided by an orbital shaker. For BNC production, static incubations at 28 °C were performed in Erlenmeyers flasks containing 4.0% w/v glycerol and corn steep liquor respectively, and keeping a flask/autoclaved medium v/v ratio of 5:1. After 14 days bacterial nanocellulose pellicles were harvested, rinsed with water to remove the culture medium, and homogenized in a blender for 5 min. The microfibrils thus obtained were treated for 14 h in a 5% w/v KOH solution in order to eliminate the bacterial cells from the cellulose matrix, and then rinsed with water till neutralization.

2.4. Organocatalytic esterification of BNC

Homogenized bacterial nanocellulose pellicles (0.5 g, dry weight) were solvent exchanged from water to the acylant by soaking and centrifugation (three times, 20 mL). The acylant (0.53 mol, i.e. 30 mL of acetic acid or 40 mL of propionic acid), tartaric acid (0.47 g) and soaked BNC were mixed in an oven-dried 100 mL glass flask equipped with a magnetic stir bar, and a reflux condenser to prevent the loss of the acylant. The mixture was heated to 120 °C under continuous agitation in a thermostatized oil bath. When the mixture achieved the target temperature, all tartaric acid dissolved and this was considered as the beginning of reaction. Esterification was run for different reaction times (1, 3, 4, 5, 6 and 8 h). After the chosen reaction time, the mixture was allowed to cool down to room temperature, and the solid product was separated by vacuum filtration in a Buchner funnel. Several washings of the recovered solid with distilled water were performed in order to guarantee the removal of the catalyst and the unreacted acid.

The acyl content of the esterified nanofibers was determined by heterogeneous saponification and back titration with HCl, as an adaptation of the approach used for determining the acyl content in cellulose acetate (ASTM D871-96, Standard Test Methods of Testing Cellulose Acetate). With this purpose, esterified BNC samples were made into pellicles by drying, grinded under liquid nitrogen flux, and carefully dried again in order to have a precise measure of the mass of sample used in saponification. With the described sample preparation protocol the method proved simple and accurate to quantitatively assay the bulk level of substitution achieved in BNC without specific instrumentation. Dried grinded samples (0.10 g, 105 °C, 2 h) were thus transferred to 100 mL Erlenmeyers to which 10 mL of ethyl alcohol (75%) was added. Flasks were heated loosely stoppered for 30 min at 50 °C. Afterwards, the suspensions were brought to slightly basic pH by addition of a few drops of 0.1 N NaOH using phenolphthalein as indicator. Aliquots of 10 mL of 0.1 N NaOH were then added to each flask, and heated again at 50 °C for 15 min. Erlenmeyers were finally allowed to stand tightly stoppered at room temperature for 72 h. At the end of this time, the excess NaOH present in the flasks was back titrated with 0.1 N HCl, using phenolphthalein as the end-point indicator. A blank determination (grinded native BNC) was carried through the complete procedure. NaOH and HCl solutions were standardized using previously dried standard potassium hydrogen phthalate and sodium carbonate, respectively.

The acyl content was then calculated by:

$$\text{Acyl}\ \ (\%) = [(V_B - V_S) \times N_{HCl} \times M_{acyl} \times 10^{-3} \times 100]/W \qquad (1)$$

where V_B (mL) is the volume of HCl required for titration of the blank; V_S (mL) is the volume of HCl required to titrate the sample; N_{HCl} is the normality of the HCl solution; M_{acyl} is the molecular

weight of the acyl group (43 for acetyl and 57 for propionyl), and W (g) is the mass of sample used.

Using the Acyl % value, the substitution degree of esterified BNC samples was calculated by:

$$DS = (162Acyl\%)/[M_{acyl} \times 100 - ((M_{acyl} - 1)Acyl\%)] \quad (2)$$

where 162 is the molecular weight of the anhydroglucose units.

2.5. Characterization of esterified BNC

Solid-state ^{13}C NMR measurements: High-resolution ^{13}C solid-state spectra of grinded samples were recorded using the ramp {1H} → {13C} CP/MAS pulse sequence (cross-polarization and magic angle spinning) with proton decoupling during acquisition. All experiments were performed at room temperature in a Bruker Avance II-300 spectrometer equipped with a 4-mm MAS probe. The operating frequency for protons and carbons was 300.13 and 75.46 MHz, respectively. Glycine was used as an external reference for the ^{13}C spectra and to set the Hartmann-Hahn matching condition in the cross-polarization experiments. The recycling time varied from 5 to 6 s according to the sample. The contact time during CP was 2 ms for all of them. The SPINAL64 sequence (small phase incremental alternation with 64 steps) was used for heteronuclear decoupling during acquisition with a proton field H1H satisfying $\omega 1H/2\pi = \gamma HH1H = 62$ kHz. The spinning rate for all the samples was 10 kHz. The crystallinity index (CI) of chosen samples was determined by separating the C4 region of the spectrum into crystalline and amorphous peaks, and calculated by dividing the area of the crystalline peak (87–93 ppm) by the total area assigned to the C4 peak (80–93 ppm) as described elsewhere (Newman, 2004; Park, Baker, Himmel, Parrilla, & Johnson, 2010).

Fourier transform infrared spectroscopy (FTIR): Fourier transform infrared spectra of native and esterified grinded samples were acquired on an IR Affinity-1 Shimadzu Fourier Transform Infrared Spectrophotometer in transmission mode. Carefully dried (10 mg, 105 °C, 1 h) grinded samples of native and acetylated BNC were mixed with previously dried (130 °C, overnight) KBr in the ratio 1:25. The prepared pellets were further dried overnight at 105 °C and spectra were finally collected with 40 scans in the range of 4000–700 cm^{-1} with a resolution of 4 cm^{-1}. Samples were normalized against the band found at 1165 cm^{-1} assigned to the (C—O—C) link of cellulose (Ilharco, Gracia, daSilva, & Ferreira, 1997; Lee et al., 2011).

X-ray diffraction (XRD): The structure of esterified BNC grinded samples was analyzed with a Rigaku D/Max-C Wide Angle automated X-ray diffractometer with vertical goniometer. The X-ray diffraction pattern was recorded in a 2θ angle range of 10–40° at a step size of 0.02°. The wavelength of the Cu/Ka radiation source used was 0.154 nm, generated at accelerating voltage of 40 kV and a filament emission of 30 mA. In order to calculate the crystallinity index of native and esterified BNC samples Segal's method was applied (Segal, Creely, Martin, & Conrad, 1959):

$$CI = (I_{002} - I_{am})/I_{002} \times 100 \quad (3)$$

where I_{002} corresponds to the maximum intensity of the 002 lattice diffraction, and I_{am} corresponds to the intensity at $2\theta = 18°$.

Thermogravimetric analysis (TGA): Thermogravimetric analysis of dried grinded samples (2.5–3 mg, 105 °C, 1 h) was conducted in a TGA-50 Shimadzu instrument. Temperature programs were run from 25 °C to 550 °C at a heating rate of 10 °C/min, under nitrogen atmosphere (30 mL/min) in order to prevent thermoxidative degradation.

Analysis of hydrophobicity: Native and esterified grinded BNC samples were qualitatively tested for hydrophobicity by water flotation in water filled vials, as well as by distribution in test tubes containing two immiscible polar/non polar liquid phases (i.e. distilled water/petroleum ether). Neat and esterified pellicles were also subjected to water drop tests, for which 10 μL water droplets were manually placed on the pellicles surface using a syringe, and the time required for complete absorption was determined.

3. Results and discussion

3.1. Organocatalytic esterification of BNC

Fig. 1 illustrates the evolution of the degree of substitution (DS) determined for acetylated and propionized BNC samples as a function of time. As it is shown, using both acids the substitution degree increased with reaction time, reaching a DS value of 0.45 for the acetylation reaction after 8 h of reaction. Using propionic acid as acylant, a lower substitution degree was achieved, reaching a DS of 0.23 in 8 h of reaction. The lower acylation level observed with propionic acid is explained in terms of a lower reactivity of this acylant due to a bulkier fatty acylium ion with higher steric hindrance. Similar tendencies have been reported previously by other authors who studied the heterogeneous esterification of cellulose nanofibers with acylants of different chain length (Uschanov et al., 2011; Tomé et al., 2011; Lee et al., 2011). The contribution of the uncatalyzed reaction was in all cases lower than 10% of the measured DS.

Literature dealing with cellulose nanofibers esterification by other methodologies has demonstrated that for a number of applications low acyl contents have succeeded in altering cellulose nanofibers properties in the desired way. Nogi et al. (2006), prepared a nanocomposite consisting of an acrylic resin reinforced with acetylated BNC nanofibers with a DS of 0.17. The authors observed that the DS achieved effectively reduced the hygroscopicity of BNC nanocomposites and improved thermal degradation resistance regarding transparency. In the surface acetylation of bacterial cellulose nanofibers using perchloric acid as catalyst, by varying the volume of acylant used Ifuku et al. (2007) obtained acetylated nanofibers with DS in the 0–1.76 interval, which were also used as acrylic resins reinforcement. The authors demonstrated that the moisture content of the nanocomposites was minimized at intermediate DS, i.e. 0.45–0.56, which they explained in terms of two opposite effects: change in nanofibers surface hydrophobicity and water penetration into the internal spaces of the esterified nanofibers upon bulky ester groups introduction.

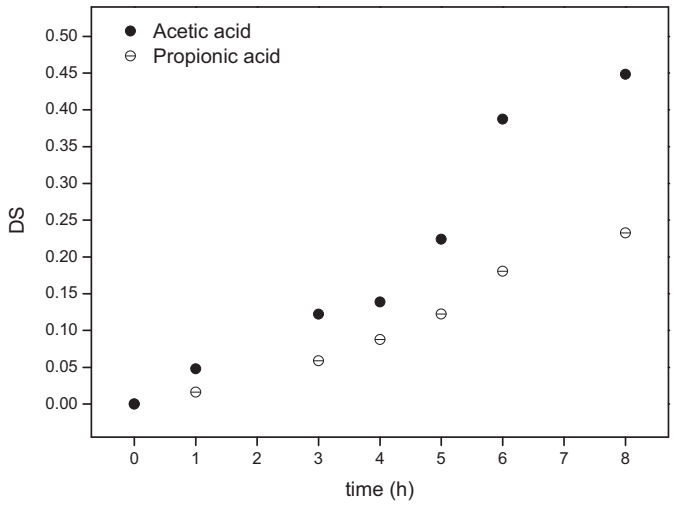

Fig. 1. Organocatalytic esterification of bacterial nanocellulose using acetic acid and propionic acid as acylants, 120 °C.

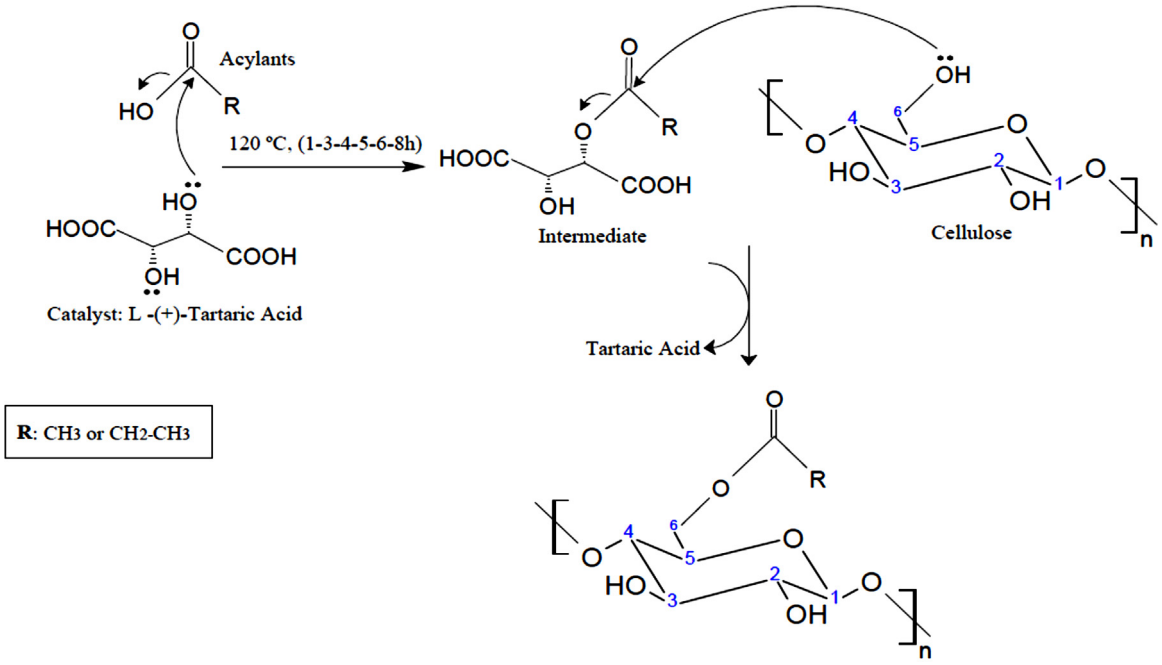

Scheme 1. Proposed mechanism for the esterification of bacterial cellulose nanofibers with acetic and propionic acids catalyzed by L-tartaric acid.

Although it has not been completely elucidated, the catalytic mechanism of esterifications catalyzed by α-hydroxy acids such as tartaric acid, has been proposed to proceed analogously to that of lipase/esterase-catalyzed reactions (Domínguez de María, 2010). According to the mechanism proposed, the acetylation and propionization reactions described herein (Scheme 1) initiate with a nucleophilic attack of the acylant by the hydroxyl group of tartaric acid. The intermediate formed is then further nucleophilically attacked by the hydroxyl groups of bacterial cellulose nanofibers, resulting in transesterification (Domínguez de María, 2010; Hafrén & Córdova, 2005).

3.2. CP/MAS ^{13}C NMR spectroscopy

Esterification of BNC by the proposed organocatalytic methodology was confirmed by use of CP/MAS ^{13}C NMR spectroscopy. Fig. 2 shows the CP/MAS ^{13}C NMR spectra obtained for native, acetylated (DS = 0.22), and propionized (DS = 0.18) BNC. Native BNC spectrum showed carbon peaks typical of cellulose I, i.e. C1: 105 ppm, C4: 89 ppm, C4′: 84 ppm, cluster C2–C3–C5: 70–80 ppm, C6: 65.3 ppm, and C6′: 62.7 ppm (Earl & VanderHart, 1980). As the esterification reaction proceeded, several new resonances appeared on the spectra (Fig. 2b and c). In the spectrum of the acetylated BNC a new peak was observed at 174 ppm, assignable to the resonance of the carbonyl ester peak. For BNC esterification with propionic acid this signal was observed at 176.2 ppm. Both samples also showed the appearance of new signals between 9 and 30 ppm, which arose from the terminal methyl carbons of acetic (21.3 ppm) and propionic acid (9.6 ppm) (Yamamoto, Horrii, & Hirai, 2005). The signal observed at 27 ppm in the propionized sample corresponds to CH_2. Signals attributable to tartaric acid acting as grafting molecule were not observed.

Crystalline and disordered components of cellulose are detected in solid-state ^{13}C NMR spectra as downfield and upfield lines for the C4 or C6 carbons, respectively (Yamamoto et al., 2005; Jandura, Kokta, & Riedl, 2000). As shown in Fig. 2, native BNC exhibited broad non-crystalline resonances centered at 84 and 62.7 ppm (upfield lines, i.e. C4′ and C6′, respectively). Downfield signals centered at 89 and 65.3 ppm (C4 and C6, respectively) have been assigned to ordered cellulose structures (Atalla & VanderHart, 1999;

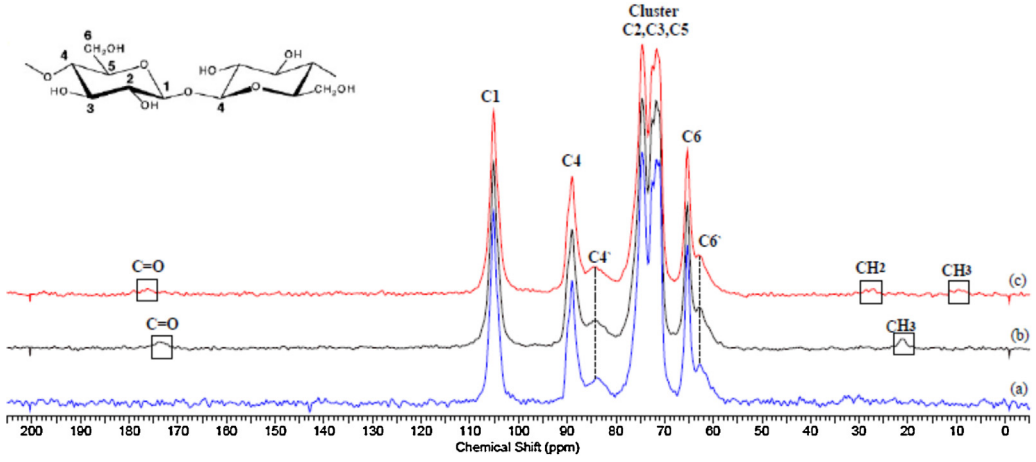

Fig. 2. CP/MAS ^{13}C NMR spectra of neat and esterified BNC samples. (a) Neat BNC, (b) acetylated BNC–DS = 0.22 and (c) propionized BNC–DS = 0.18.

Table 1
Crystallinity index of neat and esterified BNC calculated by Newman's (NMR) and 634 Segal's (XRD) method.

Sample	CI_{NMR} (%)	CI_{XRD} (%)
Native BNC	71.8	91.8
Acetylated BNC, DS = 0.14	–	90.1
Acetylated BNC, DS = 0.22	72.3	–
Acetylated BNC, DS = 0.45	–	91.9
Propionized BNC, DS = 0.09	–	92.3
Propionized BNC, DS = 0.18	69.0	–
Propionized BNC, DS = 0.23	–	90.7

Park et al., 2010). The crystallinity index of native, acetylated (DS = 0.22) and propionized BNC (DS = 0.18) was calculated using the peak separation method of Newman (2004), by dividing the area of the crystalline peak by the total area of assigned to the C4 peaks. The CI values obtained suggested that no significant change in the crystallinity of BNC took place during esterification (Table 1, CI_{NMR}).

3.3. FTIR spectroscopy

BNC esterification was further qualitatively confirmed by FTIR spectroscopy of acylated samples. Fig. 3 shows the FTIR spectra of acetylated and propionized BNC with chosen DS. The spectrum of native BNC was also included for comparison. Native BNC spectrum showed bands typical of cellulose I, showing the presence of hydroxyl groups (3360 cm^{-1}); C—H stretching (2895 cm^{-1}); H—O—H bending vibration of absorbed water molecules (1647 cm^{-1}); CH_2 symmetrical bending (1427 cm^{-1}); cellulose C—O—C bridges (1165 cm^{-1}); C—O bond stretching (1118 cm^{-1}); ether C—O—C functionalities (1061 cm^{-1}); and the band at 897 cm^{-1} which is typical of β-linked glucose polymers (Castro et al., 2011; Moosavi-Nasab & Yousefi, 2011; Rani, Navin, & Appaiah, 2011; Ashori, Babaee, Jonoobi, & Hamzed, 2014).

Spectra of acetylated and propionized BNC provided evidence of esterification by appearance of a new band at 1730 cm^{-1} which is assigned to the stretching of the ester carbonyl groups (C=O) introduced (Lee et al., 2011; Tomé et al., 2011; Ashori et al., 2014; Yuan et al., 2006; Braun & Dorgan, 2009). As shown in Fig. 3, in the spectra of samples with lower DS the intensity of the C=O ester was found to increase with the DS measured by saponification. On the other hand, although esterification implied substitution of a fraction of hydroxyl groups by less polar ester groups, no clear reduction of the intensity of the band associated with the vibration of OH groups located at 3300 cm^{-1} was observed. This behavior has previously been attributed to BNC derivatization occurring essentially on the accessible hydroxyl groups of the surface of the nanofibers or in the amorphous fraction of the cellulose (Lee et al., 2011). The absence of absorption at 1700 cm^{-1} attributed to carboxylic groups indicated that no unreacted acylant remained in the esterified BNC.

3.4. X-ray diffraction (XRD)

Cellulose has several crystalline polymorphisms (I, II, III, IV). Cellulose I is the crystalline polymorphism that is naturally produced by a variety of organisms, i.e. trees, plants, tunicates, algae and bacteria; and it is the crystal structure with the highest axial elastic modulus (Moon, Martini, Nairn, Simonsen, & Youngblood, 2011). Diffraction patterns obtained for native BNC, acetylated BNC (DS = 0.14 and DS = 0.45) and propionized BNC (DS = 0.09 and DS = 0.23) are shown in Fig. 4. Native BNC showed four diffraction peaks at $2\theta = 14.4^\circ$ (101), 16.7° (10-1), 22.5° (002), and 34.0° (040) which confirmed that only cellulose I was present in all samples (Vazquez, Foresti, Cerrutti, & Galvagno, 2013; Johnson Ford, Mendon, Thames, & Rawlins, 2010; Terinte, Ibbett, & Schuster, 2011; Gea et al., 2011). For the DS attained in this contribution, esterified cellulose nanofibers maintained the diffraction pattern of native BNC, with no evidence of peak shifting or appearance of new peaks. This is further evidence that the organocatalytic reaction involved essentially the OH groups on the surface or in the amorphous regions of BNC, not affecting in a great extent its ultrastructure (Tomé et al., 2011; Lee et al., 2011). The degree of crystallinity of native and modified BNC was determined using the Segal equation (Segal et al., 1959). Results included in Table 1 (CI_{XRD}), further confirmed that no significant change in BNC crystallinity took place during organic-acid-catalyzed esterification of BNC. As expected, absolute CI values differed from those obtained by NMR peak separation methods, since CI values are known to vary significantly depending on the measurement method used to determine them (Park et al., 2010; Terinte et al., 2011).

3.5. Thermogravimetric analysis (TGA)

Esterified BNC samples were characterized by thermogravimetric analysis to study the impact of organocatalytic esterification on

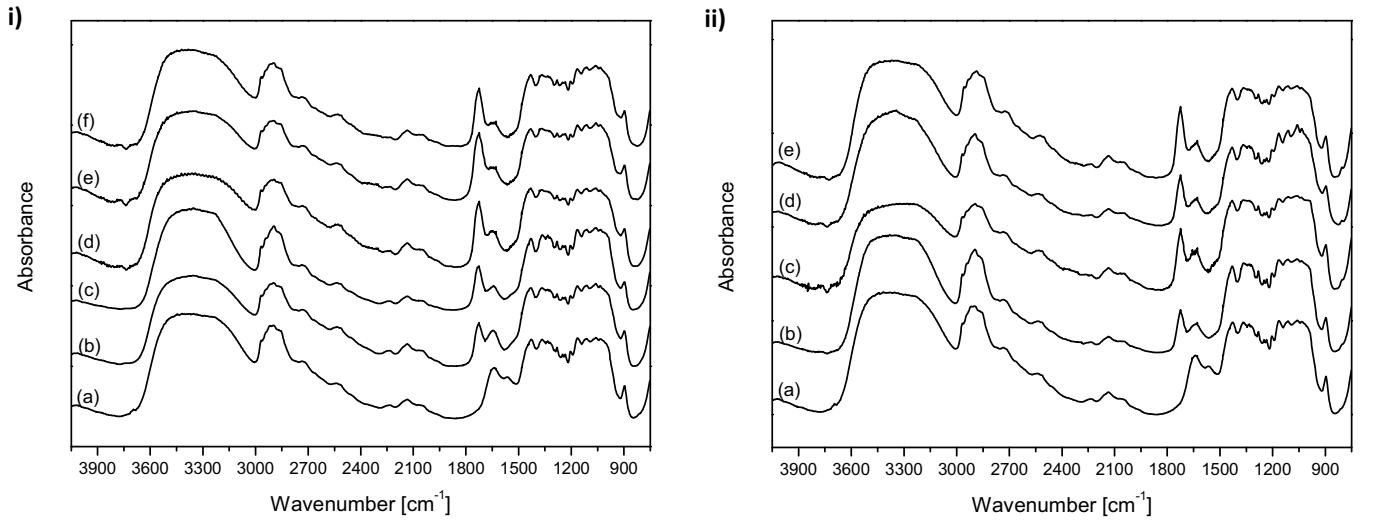

Fig. 3. FTIR spectra of neat and esterified BNC samples. Acetylated BNC (left, i): (a) neat BNC; (b) DS = 0.05; (c) DS = 0.12; (d) DS = 0.14; (e) DS = 0.39; (f) DS = 0.45. Propionized BNC (right, ii): (a) neat BNC; (b) DS = 0.06; (c) DS = 0.09; (d) DS = 0.12; (e) DS = 0.23.

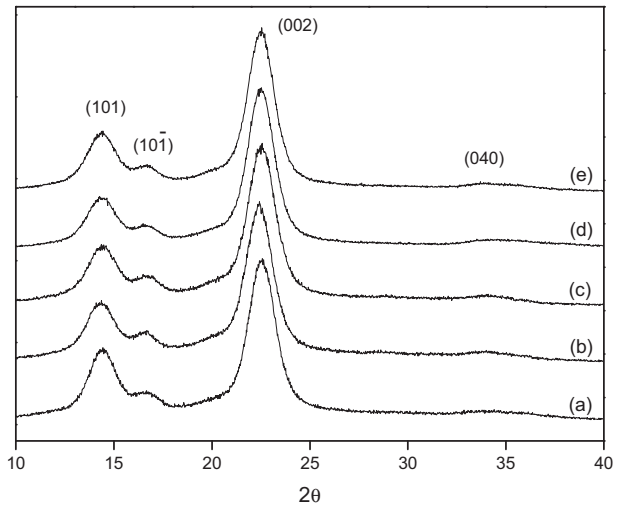

Fig. 4. X-ray diffraction pattern of neat and esterified BNC. (a) Neat BNC; (b) propionized BNC–DS = 0.09; (b) propionized BNC–DS = 0.23; (c) acetylated BNC–DS = 0.14; (d) acetylated BNC–DS = 0.45. For clarity purposes, baselines of XRD patterns have been moved up in the *y* axes.

the thermal properties of BNC. Fig. 5 shows the TG and DTG curves obtained for (i) acetylated BNC and (ii) propionized BNC samples with increasing DS. DTG data have been normalized with respect to the initial sample mass, and results have been moved up in the y axes for clarity purposes. The TG and DTG curves of native BNC have also been included for comparison.

Neat BNC pyrolysis showed a single weight loss stage, with an extrapolated onset temperature (T_{onset}) of 313 °C. T_{onset} was calculated as the intersection of the extrapolated pre-decomposition ordinate value and a tangential line drawn to the point of steepest slope of the weight loss curve in the decomposition region. According to DTG data, the maximum weight loss rate of neat BNC (T_{max}) took place at 329 °C. Thermogravimetric data of neat BNC showed a minimal weight loss assignable to BNC dehydration (2.3%), due to sample preconditioning at 105 °C during 1 h. The measured weight loss (%) during samples' preconditioning decreased as the DS of the samples increased, which was a consequence of the effect of esterification on BNC hydrophilicity.

As it is shown in Fig. 5-i, acetylated bacterial cellulose nanofibers descomposed in a single step process. Irrespectively of acylation level achieved, acetylated nanofibers started to decompose at

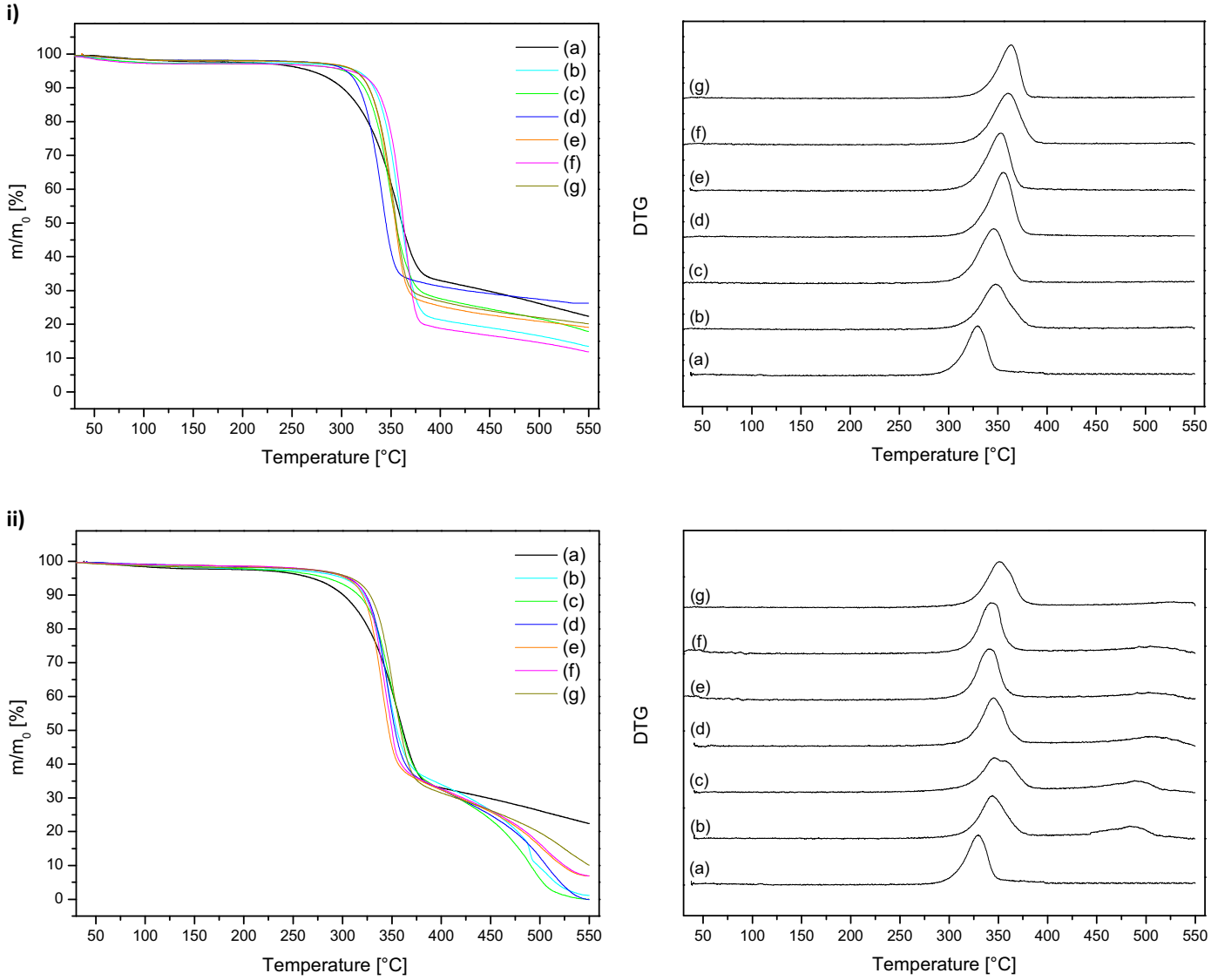

Fig. 5. TG and DTG curves of neat and esterified BNC samples. (i) Acetylated BNC: (a) neat BNC; (b) DS = 0.05; (c) DS = 0.12; (d) DS = 0.14; (e) DS = 0.22; (f) DS = 0.39; (g) DS = 0.45. (ii) Propionized BNC: (a) neat BNC; (b) DS = 0.02; (c) DS = 0.06; (d) DS = 0.09; (e) DS = 0.12; (f) DS = 0.18; (g) DS = 0.23.

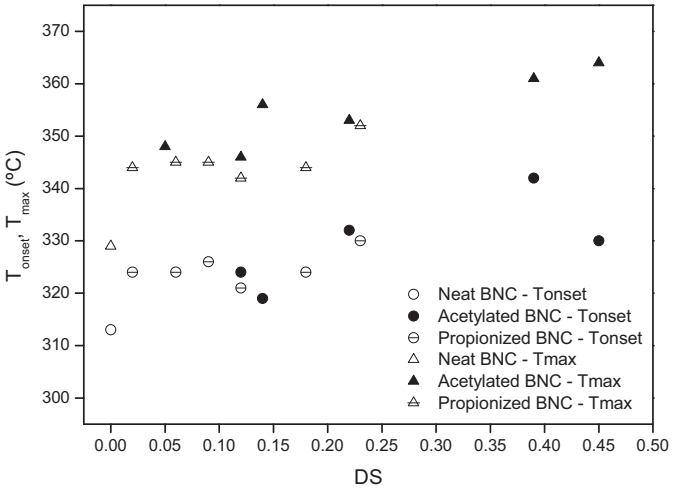

Fig. 6. T_{onset} (°C) and T_{max} (°C) values calculated for neat and esterified BNC samples with increasing DS.

substantially higher temperatures than neat BNC, with T_{onset} values that were found to increase with the DS of the sample. T_{max} values of acetylated samples also showed a positive correlation with DS. Similar tendencies were found for propionized BNC (Fig. 5-i). The increase of T_{onset} and T_{max} with the DS of acetylated and propionized samples is illustrated in Fig. 6. Results included in Fig. 6 also suggested that the length of the ester group introduced showed no significant effect on the T_{onset} and T_{max} values registered for acetylated and propionized samples with similar DS. Higher thermal stability of modified celluloses for increasing substitution degrees has previously been reported (Jandura, Riedl, & Kokta, 2000; Morgado & Frollini, 2011; Uschanov et al., 2011). Increased thermal stability of esterified samples has been attributed to the replacement of hydroxyl groups by more stable ester groups (Ashori et al., 2014; Lin, Huang, Chang, Feng, & Yu, 2011).

Among the methodologies used in the literature to heterogeneously esterify BNC, a number of authors have reported a reduction in the thermal stability of cellulose nanoparticles upon modification, characterized by onset and maximum temperature decomposition peaks found at lower temperatures than those of neat BNC (Tomé et al., 2011; Uschanov et al., 2011; Lee et al., 2011). The mentioned behavior was attributed to the reduction of cellulose crystallinity induced by esterification, and, less frequently, to the high liability of the ester linkages introduced in the cellulose structure, or to the reduced number of effective hydrogen bonds remaining among BNC nanofibers upon esterification (Tomé et al., 2011; Uschanov et al., 2011; Lee et al., 2011). In this context, the increase in thermal stability of BNC shown in Fig. 5 is in agreement with previous characterization data which evidenced that the organocatalytic esterification of cellulose nanofibers took place in their outmost layers, while keeping the ultrastructure unaffected. Specially when used as reinforcement for polymers whose melting processing require elevated temperatures, it is important that alterations of the surface chemistry of cellulose nanofibers do not decrease the onset temperature of thermal degradation (Braun & Dorgan, 2009).

In the case of propionized BNC samples a second high temperature decomposition peak was observed in the 430–550 °C range (Fig. 5-i). The DTG peak was the result of a second thermal degradation step registered in TG curves of propionized samples, which led to weight residues fractions much lower than those observed for neat BNC in the same temperature interval. The behavior observed suggested that organocatalytic propionization induced changes that increased the volatility of the solid residue of BNC samples at high temperatures. Further studies on the nature and reasons for the mentioned effects of organocatalytic propionization of BNC are currently going on.

3.6. Surface hydrophobicity

Grinded acetylated and propionized BNC samples were qualitatively tested for hydrophobicity by water flotation, distribution in polar/non-polar biphasic systems, and water drop tests. All assays confirmed that acetate or propionate groups covalently attached to the surface of BNC altered its polarity. Sample distribution in test tubes containing equal volumes of distilled water and petroleum ether (0.67 g/mL) is illustrated in Fig. 7 for chosen samples. When added to the biphasic liquid system, native BNC fell to the lower aqueous phase, absorbed water and sank immediately to the bottom of the test tube. Contrarily, acetylated (DS = 0.45) and propionized (DS = 0.23) BNC grinded samples fell across the non polar phase and remained floating in the non-polar/polar interphase without crossing to the aqueous phase (Fig. 7c and f, respectively). The described sample distribution did not change upon vertically shaking of test tubes. For both acylants, esterified samples with lower DS showed intermediate behaviors (Fig. 7b and e, respectively). In water flotation tests, samples were placed on the surface of water-filled vials. In the case of native BNC the sample absorbed water and sank immediately to the vial bottom. In contrast, esterified samples corresponding to DS = 0.45 (acetylated BNC) and DS = 0.23 (propionized BNC), did not absorb water and remained floating in the water surface (data not shown). In water drop tests 10 μL water droplets were manually placed on the surfaces of native, acetylated (DS = 0.14) and propionized (DS = 0.12) BNC pellicles. Fig. 7g–i shows the appearance of the droplets after

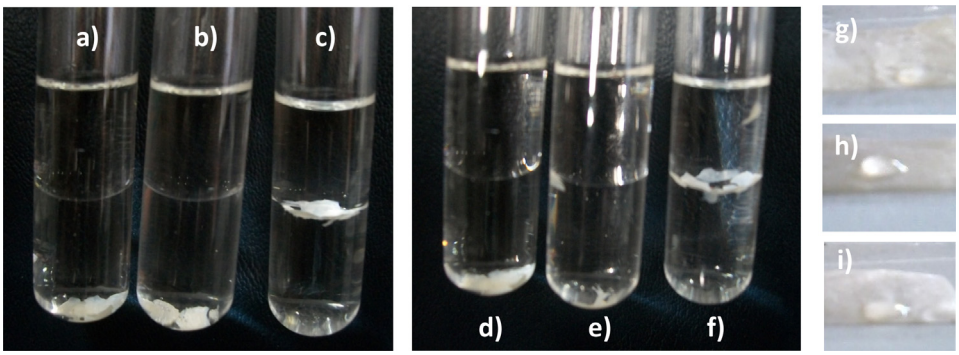

Fig. 7. Surface hydrophobicity assays. (a, d, g) Neat BNC; (b) acetylated BNC–DS = 0.14; (c) acetylated BNC–DS = 0.45; (e) propionized BNC–DS = 0.09; (f) propionized BNC–DS = 0.23; (h) acetylated BNC–DS = 0.14; (i) propionized BNC–DS = 0.12.

10 seconds. Whereas native BNC surface immediately absorbed the water droplet (Fig. 7g), a significant hydrophobicity of samples surface was observed in esterified pellicles even at relatively low DS. In the case of the acetylated pellicle (DS = 0.14, Fig. 7h), it took 38–40 min to completely absorb the drop, whereas in the case of propionized BNC (DS = 0.12, Fig. 7i) 37–39 min were required.

4. Conclusion

A simple environmental friendly esterification route to confer hydrophobicity to cellulose nanofibers was applied to the acetylation and propionization of bacterial cellulose nanofibers. The protocol applied was characterized by the use of a non-toxic natural-origin catalyst and the absence of cosolvent. By controlling the esterification time interval acetylated and propionized cellulose nanofibers with varying DS could be easily obtained. The esterification reaction was further confirmed by solid-state CP/MAS ^{13}C NMR and FTIR spectroscopy. XRD and TGA were used to monitor the effect of esterification on the crystallinity and thermal properties of BNC. Esterified BNC samples showed increased thermal stability in terms of T_{onset} and T_{max}, and no crystallinity reduction with respect to native BNC. Besides, hydrophobicity tests confirmed the change in cellulose microfibrils polarity. NMR, FTIR, XRD and TGA results all contributed to the conclusion that the organocatalytic acetylation and propionization of BNC occurred mainly in the surface of cellulose nanofibers. Surface esterification of cellulose nanofibers is desirable for improving the compatibility of the cellulosic substrate with apolar matrices, while preserving the crystalline ultrastructure of cellulose. In this context, the organocatalytic route proposed appears as a promising ecofriendly approach for tailoring the surface properties of BNC to be used for example in the development of biodegradable polyester reinforced nanocomposites. Further assays, aiming to assert the effect of reaction conditions to be used to tune the extent of esterification achieved in BNC and other cellulose nanoparticles substrates are currently in progress.

5. Ackowledgements

The authors acknowledge Consejo Nacional de Investigaciones Científicas y Técnicas (CONICET-PIP 11220110100608), University of Buenos Aires (UBACYT 20020090100065), and Agencia Nacional de Promoción Científica y Tecnológica (PICT 1957 2012 – PRESTAMO BID) for financial support.

References

Ashori, A., Babaee, M., Jonoobi, M., & Hamzed, Y. (2014). Solvent-free acetylation of cellulose nanofibers for improving compatibility and dispersion. *Carbohydrate Polymers*, *102*, 369–375.

Atalla, R. H., & VanderHart, D. L. (1999). The role of solid state 13C NMR spectroscopy in studies of the nature of native celluloses. *Solid State Nuclear Magnetic Resonance*, *15*, 1–19.

ASTM D871-96, Standard test methods of testing cellulose acetate.

Berlioz, S., Molina-Boisseau, S., Nishiyama, Y., & Heux, L. (2009). Gas-phase surface esterification of cellulose microfibrils and whiskers. *Biomacromolecules*, *10*, 2144–2151.

Braun, B., & Dorgan, J. R. (2009). Single-step method for the isolation and surface functionalization of cellulosic nanowhiskers. *Biomacromolecules*, *10*, 334–341.

Castro, C., Zuluaga, R., Putaux, J. L., Caroa, G., Mondragon, I., & Gañan, P. (2011). Structural characterization of bacterial cellulose produced by *Gluconacetobacter swingsii* sp. from Colombian agroindustrial wastes. *Carbohydrate Polymers*, *84*, 96–102.

Domínguez de María, P. (2010). Minimal hydrolases: Organocatalytic ring-opening polymerizations catalyzed by naturally occurring carboxylic acids. *ChemCatChem*, *2*, 487–492.

Earl, W. L., & VanderHart, D. L. (1980). High resolution, magic angle sample spinning 13C NMR of solid cellulose I. *Journal of the American Chemical Society*, *102*, 3251–3252.

Gea, S., Reynolds, C. T., Roohpour, N., Wirjosentono, B., Soykeabkaew, N., Bilotti, E., et al. (2011). Investigation into the structural, morphological, mechanical and thermal behaviour of bacterial cellulose after a two-step purification process. *Bioresource Technology*, *102*, 9105–9110.

Hafrén, J., & Córdova, A. (2005). Direct organocatalytic polymerization from cellulose fibers. *Macromolecular Rapid Communications*, *26*, 82–86.

Hu, W., Chen, S., Xu, Q., & Wang, H. (2011). Solvent-free acetylation of bacterial cellulose under moderate conditions. *Carbohydrate Polymers*, *83*, 1575–1581.

Hubbe, M. A., Rojas, O. J., Lucia, L. A., & Sain, M. (2008). Cellulosic nanocomposites: A review. *BioResources*, *3*, 929–980.

Ifuku, S., Nogi, M., Abe, K., Handa, K., Nakatsubo, F., & Yano, H. (2007). Surface modification of bacterial cellulose nanofibers for property enhancement of optically transparent composites: Dependence on acetyl-group DS. *Biomacromolecules*, *8*, 1973–1978.

Ilharco, L. M., Gracia, R. R., daSilva, J. L., & Ferreira, L. F. V. (1997). Infrared approach to the study of adsorption on cellulose: Influence of cellulose crystallinity on the adsorption of benzophenone. *Langmuir*, *13*, 4126–4132.

Jandura, P., Kokta, B. V., & Riedl, B. (2000). Fibrous long-chain organic acid cellulose esters and their characterization by diffuse reflectance FTIR spectroscopy, solid-state CP/MAS ^{13}C-NMR, and W-ray diffraction. *Journal of Applied Polymer Science*, *78*, 1354–1365.

Jandura, P., Riedl, B., & Kokta, B. V. (2000). Thermal degradation behaviour of cellulose fibers partially esterified with some long chain organic acids. *Polymer Degradation and Stability*, *70*, 387–394.

Johnson Ford, E. N., Mendon, S. K., Thames, S. F., & Rawlins, J. W. (2010). X-ray diffraction of cotton treated with neutralized vegetable oil-based macromolecular crosslinkers. *Journal of Engineered Fibers and Fabrics*, *5*, 10–20.

Lee, K.-Y., Quero, F., Blaker, J. J., Hill, C. A. S., Eichhorn, S. J., & Bismarck, A. (2011). Surface only modification of bacterial cellulose nanofibers with organic acids. *Cellulose*, *18*, 595–605.

Lin, N., Huang, J., Chang, P. R., Feng, J., & Yu, J. (2011). Surface acetylation of cellulose nanocrystal and its reinforcing function in poly(lactic acid). *Carbohydrate Polymers*, *83*, 1834–1842.

Moon, R. J., Martini, A., Nairn, J., Simonsen, J., & Youngblood, J. (2011). Cellulose nanomaterials review: Structure, properties and nanocomposites. *Chemical Society Reviews*, *40*, 3941–3994.

Moosavi-Nasab, M., & Yousefi, A. (2011). Biotechnological production of cellulose by *Gluconacetobacter xylinus* from agricultural waste. *Iranian Journal of Biotechnology*, *9*, 94–101.

Morgado, D. L., & Frollini, E. (2011). Thermal decomposition of mercerized linter cellulose and its acetates obtained from a homogeneous reaction. *Polímeros*, *21*, 111–117.

Newman, R. H. (2004). Homogeneity in cellulose crystallinity between samples of *Pinus radiata* wood. *Holzforschung*, *58*, 91–96.

Nogi, M., Abe, K., Handa, K., Nakatsubo, F., Ifuku, S., & Yano, H. (2006). Property enhancement of optically transparent bionanofiber composites by acetylation. *Applied Physics Letters*, *89*, 233123-1–233123-3.

Park, S., Baker, J. O., Himmel, M. E., Parilla, P. A., & Johnson, D. K. (2010). Cellulose crystallinity index: Measurement techniques and their impact on interpreting cellulose performance. *Biotechnology for Biofuels*, *3*, 1–10.

Rani, M. U., Navin, K. R., & Appaiah, K. A. A. (2011). Statistical optimization of medium composition for bacterial cellulose production by *Gluconacetobacter hansenii* UAC09 using coffee cherry husk extract—an agro-industry waste. *Journal of Microbiology and Biotechnology*, *21*, 739–745.

Sassi, J.-F., & Chanzy, H. (1995). Ultrastructural aspects of the acetylation of cellulose. *Cellulose*, *2*, 111–127.

Segal, L., Creely, J. J., Martin, A. E., & Conrad, C. M. (1959). An empirical method for estimating the degree of crystallinity of native cellulose using the X-ray diffractometer. *Textile Research Journal*, *29*, 786–794.

Siqueira, G., Bras, J., & Dufresne, A. (2010). Cellulosic bionanocomposites: A review of preparation, properties and applications. *Polymers*, *2*, 728–765.

Siro, I., & Plackett, D. (2010). Microfibrillated cellulose and new composite materials: A review. *Cellulose*, *17*, 459–494.

Terinte, N., Ibbett, R., & Schuster, K. C. (2011). Overview on native cellulose and microcrystalline cellulose I structure studied by X-ray diffraction (WAXD): Comparison between measurement techniques. *Lenzinger Berichte*, *89*, 118–131.

Tomé, L. C., Freire, M. G., Rebelo, L. P. N., Silvestre, A. J. D., Neto, C. P., Marrucho, I. M., et al. (2011). Surface hydrophobization of bacterial and vegetable cellulose fibers using ionic liquids as solvent media and catalysts. *Green Chemistry*, *13*, 2464–2470.

Tupa, M., Maldonado, L., Vázquez, A., & Foresti, M. L. (2013). Simple organocatalytic route for the synthesis of starch esters. *Carbohydrate Polymers*, *98*, 349–357.

Uschanov, P., Johansson, L.-S., Maunu, S. L., & Laine, J. (2011). Heterogeneous modification of various celluloses with fatty acids. *Cellulose*, *18*, 393–404.

Vazquez, A., Foresti, M. L., Cerrutti, P., & Galvagno, M. A. (2013). bacterial cellulose from simple and low cost production media by *Gluconacetobacter xylinus*. *Journal of Polymers and the Environment*, *21*, 545–554.

Yamamoto, H., Horrii, F., & Hirai, A. (2005). Structural studies of bacterial cellulose trough the solid-phase nitration and acetylation by CP/MAS ^{13}C NMR spectroscopy. *Cellulose*, *13*, 327–342.

Yuan, H., Nishiyama, Y., Wada, M., & Kuga, S. (2006). Surface acylation of cellulose whiskers by drying aqueous emulsion. *Biomacromolecules*, *7*, 696–700.